Pharmaceutical Research, Vol. 23, No. 4, April 2006 (© 2006)
DOI: 10.1007/s11095-006-9778-7

Research Paper

Production of Soluble and Active Transferrin Receptor-Targeting Single-Chain Antibody using *Saccharomyces cerevisiae*

Benjamin J. Hackel,[1] Dagang Huang,[1] Jennifer C. Bubolz,[1] Xin X. Wang,[1] and Eric V. Shusta[1,2]

Received August 16, 2005; accepted December 16, 2005

Purpose. This study describes the soluble production, purification, and functional testing of an anti-transferrin receptor single-chain antibody (OX26 scFv) using the yeast *Saccharomyces cerevisiae*.
Methods. The yeast secretion apparatus was optimized by modulating expression temperature, the folding environment of the endoplasmic reticulum, and gene dosage. Secreted scFv was purified using immobilized metal affinity chromatography, and tested for binding and internalization into the RBE4 rat brain endothelial cell line.
Results. Secretion of OX26 scFv was optimal when expression was induced at 20°C. Co-overexpression of heavy chain binding protein and protein disulfide isomerase elevated scFv expression levels by 10.4 ± 0.3-fold. Optimization of scFv gene dosage increased secretion by 7.1 ± 0.2-fold, but the overall benefits of binding protein and protein disulfide isomerase overexpression were diminished. Purified OX26 scFv yields of 0.5 mg/L secreted protein were achieved, and the scFv was actively internalized into RBE4 cells with a pattern similar to that observed with intact OX26 monoclonal antibody.
Conclusions. The optimized *S. cerevisiae* expression system is amenable to production of soluble and active brain targeting OX26 scFv, and the yeast-produced scFv has potential for the targeting and delivery of small molecules, proteins, or drug carriers across the blood–brain barrier (BBB).

KEY WORDS: blood–brain barrier; drug targeting; single-chain antibody; yeast.

INTRODUCTION

The blood–brain barrier (BBB) provides a formidable obstacle for the delivery of brain therapeutics as it separates the bloodstream from the brain parenchyma. The absence of fenestrae and the presence of epithelial-like tight junctions render the BBB impermeable to all molecules unless they are small (<500 Da) and lipophilic (1). Even if a brain drug possesses these characteristics, efflux transporters such as P-glycoprotein (MDR1) and members of the multidrug resistance-associated protein family (MRP) limit brain uptake (2). Because of these BBB attributes, many small molecules are excluded from the brain interior, and the rapidly expanding collections of protein and gene medicines are almost exclusively BBB-impermeable.

A BBB delivery strategy that has shown considerable promise makes use of receptor-mediated transcytosis systems such as the insulin and transferrin receptors that are present at high levels in BBB endothelium such as those involving the insulin and transferrin receptors (3,4). Appropriately targeted antibodies that recognize extracellular epitopes of the insulin and transferrin receptors can act as artificial transporter substrates that are effectively transported across the BBB and deposited into the brain interstitium via the transendothelial route. Additionally, when conjugated to drugs or drug carriers of various size and composition, the BBB targeting antibodies mediate brain uptake of these therapeutic cargos. As an example, noninvasive transport of small molecules such as methotrexate has been achieved using anti-transferrin receptor antibodies (5). Proteins such as nerve growth factor (6), brain-derived neurotrophic factor (7), and basic fibroblast growth factor (8) have also been delivered to the brain after intravenous administration by using an anti-transferrin receptor antibody. The latter two cases promoted reduction in stroke volume in rat middle cerebral artery occlusion models. In addition, liposomes (9) and liposomes loaded with genes (10) have been delivered to the brain *in vivo* using anti-transferrin receptor antibodies. Gene-containing antibody-targeted liposomes have been targeted to rat brain for restoration of tyrosine hydroxylase activity in an experimental Parkinson's disease model (11) and have been targeted to primate brain using a humanized anti-insulin receptor antibody (12). Finally, anti-transferrin receptor conjugated nanoparticles have been produced (13). Taken together, these results indicate the potential utility of antibody-targeted transcytosis systems for noninvasive trafficking of drugs into the brain.

Single-chain antibody (scFv) fragments consisting solely of the heavy and light chain variable regions of an intact antibody often retain much of their antigen binding affinity

[1] Department of Chemical and Biological Engineering, University of Wisconsin-Madison, 1415 Engineering Drive, Madison, Wisconsin 53706, USA.
[2] To whom correspondence should be addressed. (e-mail: shusta@engr.wisc.edu)

and specificity. As an alternative to intact monoclonal antibodies, these fragments may have advantages for certain applications such as immunotoxin targeting as a consequence of their reduced size (~30 kDa) and enhanced clearance rates from the body. In addition, scFv fragments can be readily produced in scalable cost-effective microbial systems that include bacteria (14,15) and yeast (16,17). Like intact antibodies, scFvs can be used to decorate drug-containing particles as demonstrated by an anti-ErbB2 scFv that promotes targeting and internalization of liposomes into cancer cells (18).

Prior studies have indicated that an scFv (OX26) against the rat transferrin receptor avidly binds the transferrin receptor and mediates brain uptake *in vivo* when produced as a fusion to streptavidin (19). Such targeting and therapeutic bifunctionality represents another advantage of the scFv format. The targeting scFv can either be fused to streptavidin and coupled to a biotinylated drug or drug carrier, or instead scFv could be directly fused to a protein therapeutic of interest. However, previous attempts to produce the OX26 scFv have yielded mixed results. The OX26 scFv–streptavidin fusion protein has been produced in *Escherichia coli* in the form of inclusion bodies, but it required refolding (19). Attempts to produce soluble, secreted OX26 scFv in the yeast *Pichia pastoris* yielded an scFv product with incomplete leader sequence processing and hyperglycosylation (20).

In order to overcome the OX26 expression problems observed in *E. coli* (insoluble inclusion bodies) and *P. pastoris* (incomplete processing and potentially immunogenic glycosylation), this investigation examined the possibility of producing OX26 scFv in the yeast *Saccharomyces cerevisiae*. OX26 scFv was subcloned into a multipurpose expression vector that has been repeatedly validated for single-chain antibody expression (16,17). Optimization of the folding environment of yeast by co-overexpressing chaperones and foldases led to much-improved secretion of soluble OX26 scFv that was completely processed. OX26-mediated endocytosis into a rat brain endothelial cell line confirmed the activity of the purified protein. This *S. cerevisiae* production system is therefore amenable to production of BBB targeting scFv and offers an attractive alternative to the previously described bacterial and *P. pastoris* systems.

MATERIALS AND METHODS

Yeast and Bacteria Strains

E. coli strains DH5α (Invitrogen, Carlsbad, CA, USA) and XL1-Blue (Stratagene, La Jolla, CA, USA) were used for plasmid construction. Plasmids were transformed into *S. cerevisiae* strains BJ5464 (*α ura3-52 trp1 leu2Δ1 his3Δ200 pep4*::*HIS3 prb1Δ1.6R can1 GAL*) (Yeast Genetic Stock Center, Berkeley, CA USA) and YVH10 using the lithium acetate method (21). Yeast strainYVH10 is BJ5464 containing an additional copy of the yeast protein disulfide isomerase (yPDI) gene integrated in tandem with the endogenous gene (22). Transformants were selected on minimal SD medium (2% dextrose, 0.67% yeast nitrogen base) buffered at pH 6.6 with 50 mM sodium phosphate and containing either 1% casamino acids (lacking tryptophan and uracil) or 2x SCAA amino acid supplement (190 mg/L Arg, 108 mg/L Met, 52 mg/L Tyr, 290 mg/L Ile, 440 mg/L Lys, 200 mg/L Phe, 1260 mg/L Glu, 400 mg/L Asp, 480 mg/L Val, 220 mg/L Thr, 130 mg/L Gly, lacking leucine, tryptophan, and uracil). 200 mg/L leucine, 20 mg/L tryptophan, and 20 mg/L uracil were supplemented when necessary for proper auxotrophic selection. Yeast transformed with linearized pITY-OX26 were selected using YPD medium (1% yeast extract, 2% peptone, 2% dextrose) containing varying levels of geneticin from 150 to 1,000 mg/L (Sigma, St. Louis, MO, USA). Geneticin-resistant yeast clones were screened for protein secretion levels, and the optimal integrated strain was used for additional study. When necessary, appropriate null plasmids were introduced into yeast strains such that comparison of secretion levels between strains could be made under identical growth and induction conditions.

Secretion and Overexpression Plasmids

Two centromere-based (CEN) low copy plasmids having different auxotrophic markers, pRS314-GALOX26 (*TRP1*) and pRS316-GALOX26 (*URA3*), were constructed for all plasmid-based expression studies and are uniformly referred to in the text as pRS-GALOX26. Briefly, the pRS-316 backbone, *GAL1-10* promoter, and alpha factor 3′ untranslated region were excised from pRS-GALT-LWHI (23) using the restriction enzymes *Eag*I and *Bgl*II. An oligonucleotide was inserted to add an *Eco*RI site downstream of the *Eag*I site. Subsequently, the OX26 scFv open reading frame was excised from pOPE-OX26 (19) as an *Eco*RI to *Bgl*II fragment and ligated into the modified pRS-GALT backbone to produce pRS316-GALOX26. The final construct comprised of galactose inducible *GAL1-10* promoter, synthetic prepro leader sequence, OX26 scFv open reading frame, c-*myc* epitope, six histidine epitope, and alpha factor untranslated region. The full expression cassette of pRS316-GALOX26 was then excised with *Kpn*I and *Sac*I and ligated to the pRS-314 backbone to produce pRS314-GALOX26. The plasmid pITY-OX26 was constructed for chromosomal integration. The OX26 expression cassette was excised from pRS316-GALOX26 and ligated into the pITY backbone (24) using *Kpn*I and *Sac*I restriction sites. The plasmid was linearized by digestion with *Mfe*I prior to yeast transformation to promote integration into the Ty δ sites of the yeast chromosome (24). The removal of a kex2p protease cleavage site near the carboxy terminus of the OX26 scFv (R261G) was performed using the Quikchange™ site-directed mutagenesis kit (Stratagene, La Jolla, CA).

Constitutive rat protein disulfide isomerase (rPDI) overexpression was obtained by transformation of the 2μ plasmid pMAL5.1 (25) into BJ5464 yeast. The molecular chaperone, heavy chain binding protein (BiP), was overexpressed using the galactose-inducible CEN-based plasmids pGAL-Kar2Leu (*LEU2*) or pMR1341 (*URA3*) (26). Yeast PDI was overexpressed in the pITY-OX26 integrated yeast strains using pCT37 (27). Null plasmids, pRS-314 (*TRP1*), pRS-315 (*LEU2*), and pRS-316 (*URA3*) (28) were used as control plasmids. The antifluorescein single-chain antibody 4-4-20

was produced using the pRS-GAL4420 plasmid previously described (17).

Secretion Studies

Yeast were inoculated into 3 mL SD medium at an initial cell density corresponding to an OD_{600} of 0.1 and grown for 84 h at 30°C. Cells were collected by centrifugation and resuspended in an SG induction medium that is identical to SD except that 2% galactose replaces dextrose as the carbon source. Bovine serum albumin (1 mg/mL) was added to prevent protein adsorption losses. Secretion continued for 72 h at 20°C unless otherwise indicated. OD_{600} cell density measurements were recorded, and the cell-free supernatant was collected for Western blot analysis.

Culture supernatant was resolved by sodium dodecyl sulfate polyacrylamide gel electrophoresis (SDS-PAGE) with a 4% stacking gel and a 12.5% separating gel. Resolved proteins were electrophoretically transferred to a 0.2-μm nitrocellulose membrane (Bio-Rad, Hercules, CA, USA) using an XCell transfer apparatus (Novex, San Diego, CA, USA). Membranes were blocked overnight at 4°C in a solution of 50 g/L nonfat milk, 8 g/L NaCl, and 0.1% Tween 20, buffered to pH 7.6 with 20 mM Tris. The blocked membranes were probed with 1 μg/mL 9E10 anti c-*myc* antibody (Covance, Berkeley, CA) followed by an antimouse IgG horse radish peroxidase conjugate (Sigma). ScFv was detected using enhanced chemiluminescence and exposure to autoradiography film (ECL Hyperfilm, Amersham, Piscataway, NJ) for varying exposure times. The intensity of each band relative to the background was determined using NIH ImageJ software. The slopes of the intensity-*vs*.-exposure time curve in the unsaturated, linear range were proportional to protein concentration in the respective samples and were used for relative comparisons in secretion level.

ScFv Purification and Characterization

Yeast strain YVH10 was transformed with pRS314-GALOX26 R261G and pMR1341 plasmids. Fifty milliliters of yeast culture was grown for 72 h at 30°C in SD-SCAA and scFv secretion was induced in SG-SCAA for 72 h at 20°C. After centrifugation to remove yeast cells, the culture supernatant was dialyzed against phosphate-buffered saline (PBS; 8.0 g/L NaCl, 0.2 g/L KCl, 1.44 g/L Na_2HPO_4, 0.24 g/L KH_2PO_4, pH 8.0). The scFv was purified from the dialyzed supernatant by employing a Ni-NTA (Qiagen, Valencia, CA, USA) affinity column as previously described (29). The purified OX26 R261G scFv was resolved on a 12.5% SDS-PAGE and stained with Coomassie blue. ScFv concentration was estimated by comparing the scFv band intensity with a series of carbonic anhydrase (31 kDa) standards of known concentration.

The molecular weight of intact OX26 R261G was measured by using matrix-assisted laser desorption/ionization time-of-flight mass spectrometry (MALDI-TOF, Bruker Biflex III) (Proteomics Facility, University of Wisconsin–Madison Biotechnology Center). Prior to mass spectrometry, purified OX26 R261G was desalted with a Zeba desalt spin column (Pierce, Rockford, IL, USA). For peptide mapping studies, purified OX26 R261G was resolved on a 12.5% SDS-PAGE gel and stained with Coomassie blue. The scFv band was extracted, digested with trypsin, and analyzed by MALDI-TOF mass spectrometry (Proteomics Facility, University of Wisconsin–Madison Biotechnology Center). ExPASy Proteomics software (http://www.expasy.org) was used to identify the amino acid sequences corresponding to the assigned masses of the peptide fragments. For N-terminal sequencing, purified OX26 R261G was electrophoresed (SDS-PAGE) and transferred to a PVDF membrane (Bio-Rad). The N-terminal sequencing was subsequently performed on a Beckman-Coulter LF3000G protein sequencer using the Edman degradation method (Protein and Nucleic Acid Facility, Medical College of Wisconsin, Milwaukee, WI, USA). The glycosylation status of OX26 R261G was evaluated by incubating purified scFv with glycosidases: PNGase F or EndoHf (New England Biolabs, Ipswich, MA, USA) at 37°C for 2 h and jack bean α-mannosidase (Sigma) at 25°C for 2 h. After treatment with glycosidase, the protein was analyzed by Western blotting as described above.

RBE4 Cell Culture

RBE4, a rat brain endothelial cell line, was a kind gift from Dr. Françoise Roux (30). RBE4 cells were grown on collagen type I-coated (Sigma) tissue culture flasks and in complete growth medium containing 45% Alpha Minimum Essential Medium (α-MEM), 45% Ham's F10 medium, 10% fetal calf serum (FCS) (Invitrogen), 100 mg/L streptomycin, 100,000 units/L penicillin G, 0.3 g/L geneticin (Invitrogen), and 1 μg/L basic fibroblast growth factor (bFGF) (Roche Diagnostics, Indianapolis, IN, USA). RBE4 cells were grown to about 80% confluency on collagen type I-coated (Sigma) 24-well culture plates for immunofluorescent labeling experiments.

Immunofluorescence

OX26 R261G scFv and 4-4-20 scFv were purified as described above. For immunofluorescent labeling of RBE4 cells, about 80% confluent RBE4 cultures were blocked with 40% goat serum (Sigma-Aldrich, St. Louis, MO) in PBS containing calcium and magnesium (PBSCM: 0.15 M NaCl, 1.9 mM NaH_2PO_4, 8.1 mM Na_2HPO_4, pH 7.4, 1 mM $CaCl_2$, 0.5 mM $MgCl_2$) for 30 min at 4°C. OX26 and 4-4-20 scFv were preincubated with 10 μg/mL 9E10 (Covance, Berkeley, CA, USA) at 1:1 (v/v) ratio for 1 h at room temperature to form artificial dimers of scFv (31). This procedure yields an scFv labeling concentration of 2.4 μg/mL. RBE4 cells were washed three times with ice cold PBSCM after blocking and then incubated with OX26 scFv artificial dimer, 4-4-20 scFv artificial dimer, OX26 monoclonal antibody (10 μg/mL; Serotec, Raleigh, NC, USA), or mouse IgG2a isotype control (10 μg/mL, Sigma-Aldrich) for 1 h at 4°C. RBE4 cells were washed after the primary labeling and then incubated with antimouse IgG phycoerythrin conjugate (Sigma-Aldrich) for 30 min at 4°C. After extensive washing, RBE4 cells were either fixed immediately with 4% paraformaldehyde for 10 min on ice (4°C sample) or fixed after further incubation at

37°C for 30 min to allow internalization (37°C sample). The samples were then examined by fluorescence microscopy (Olympus IX70 fluorescence microscope).

RESULTS

Cloning of OX26 scFv into *S. cerevisiae* Expression System

The open reading frame encoding the OX26 scFv was transferred from the bacterial pOPE-OX26 expression vector (19) into the pRS-GAL series of scFv expression vectors (17) to create pRS-GALOX26 as described in detail in Materials and Methods. The resulting low copy number plasmid controls scFv expression with the galactose-inducible *GAL1-10* promoter. A synthetic prepro leader sequence directs scFv entry into and processing through the yeast secretory pathway (29,32). Carboxy-terminal c-*myc* and six histidine epitopes are present for detection and purification purposes, respectively. Subsequently, the entire expression cassette was shuttled to the δ vector system (pITY-OX26) that allows for chromosomal integration and tuning of gene copy number (24).

Optimization of OX26 scFv Secretion Levels

S. cerevisiae harboring the pRS-GALOX26 expression plasmid were used to secrete OX26 scFv to the culture medium. First, the temperature at which protein expression was induced was varied from 20 to 37°C. Induction at 20°C served to increase OX26 secretion by 4.5 ± 0.2-fold *vs.* the 37°C condition (Fig. 1). Next, the folding environment of the endoplasmic reticulum was modified with the goal of further increasing the level of OX26 secretion at 20°C. Upon overexpression of the heavy chain binding protein chaperone, BiP, OX26 secretion was increased 3.6 ± 0.4-fold (Fig. 2). Overexpression of yeast protein disulfide isomerase (PDI) through use of the YVH10 yeast strain (Materials and Methods) yielded a similar increase of 4.3 ± 1.0-fold. Overexpression of rat PDI resulted in a more modest increase of 1.8 ± 0.3-fold. Co-overexpression of both BiP and yeast PDI yielded a 10-fold improvement in the secretion levels of OX26 compared with the wild-type control yeast strains (Fig. 2).

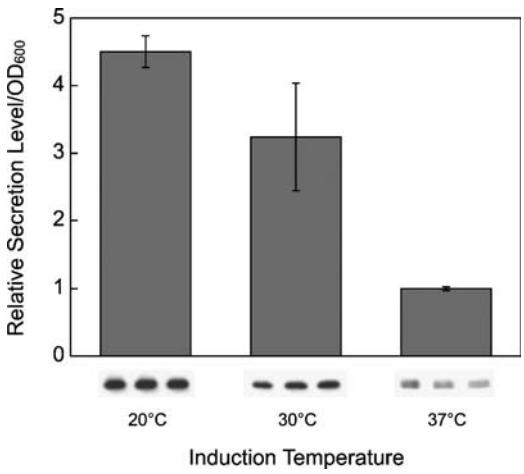

Fig. 1. Relative OX26 scFv secretion levels under different induction temperatures. The secretion levels were normalized to the 37°C induction condition. All secretion levels were normalized for cell density (OD_{600}), and representative triplicate Western blot data are given below corresponding plotted data. Absolute secretion levels are detailed in Table I.

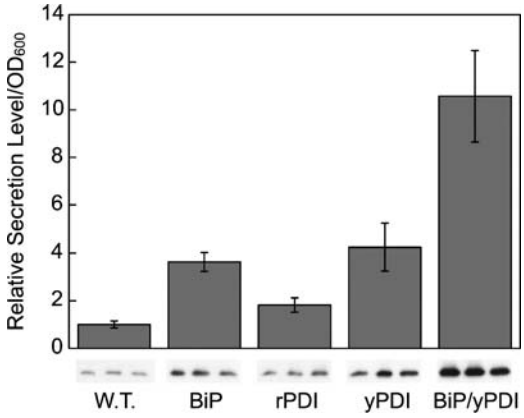

Fig. 2. Effects of BiP and PDI overexpression on OX26 scFv secretion levels. Secretion levels were normalized to those found for wild-type (W.T.) yeast strains producing OX26 scFv without BiP or yPDI overexpression. The secretion induction temperature was 20°C. BiP: heavy chain binding protein; rPDI: rat protein disulfide isomerase; yPDI: yeast protein disulfide isomerase.

The induction temperature study was repeated for the BiP and PDI co-overexpression system to ensure that 20°C was still the optimal condition for the engineered yeast strain. As Fig. 3 indicates, cooverexpression of BiP and PDI further exacerbated the observed differences in secretion level. The difference in expression level between 20 and 37°C increased from 4.5 ± 0.2- (Fig. 1) to 21.0 ± 0.6-fold for the coover-expression system (Fig. 3). In addition, Western blotting indicated that the 20°C product is completely processed yielding a single scFv band of an expected ~30 kDa size. In contrast, ~50% of the OX26 produced at 37°C retains the pro region that is normally cleaved by the kex2p protease in the Golgi apparatus, and this larger species is represented by the upper, slower migrating band (Fig. 3).

Since the pRS-GALOX26 system results in approximately 1–2 gene copies per cell on average, the gene dosage

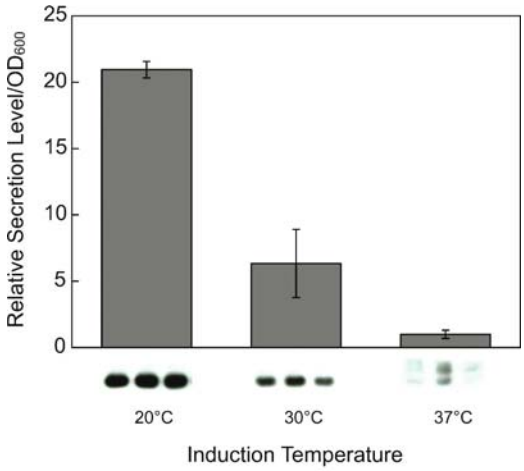

Fig. 3. Effects of induction temperature on secretion levels of OX26 scFv from yeast strains cooverexpressing BiP and yPDI. Secretion levels were normalized to those found during 37°C induction.

was tuned using the pITY-OX26 plasmid with the goal of increasing OX26 secretion. The pITY-OX26 system results in chromosomal integration of the OX26 gene at Ty δ sites in the yeast chromosome (24). The number of gene copies inserted roughly correlates with the geneticin resistance of the transformed yeast clone (24). In this way, as assessed by geneticin resistance, yeast clones harboring varying numbers of integrated copies were evaluated for OX26 scFv secretion levels. Twenty-one clones were tested by Western blotting and the highest secreting clone produced 7.1 ± 0.2 times the scFv as the nonintegrating pRS-GALOX26 plasmid system (Fig. 4). However, in contrast to the nonintegrating system, cooverexpression of BiP and PDI resulted in only small (1.4 ± 0.2) increases in scFv production. These limited increases yielded a final yeast strain having OX26 secretion levels equivalent to that found for the plasmid system with BiP and PDI cooverexpression (Fig. 4).

In addition to removing the pro region from the OX26 scFv, the yeast kex2p protease can cleave recombinant proteins at lysine–arginine sites. The OX26 scFv has such a site at the carboxy terminus immediately preceding the c-*myc* epitope (R261 (19)). This site was mutated from arginine to glycine (R261G) to prevent any carboxy-terminal proteolytic degradation mediated by the kex2p protease. This modification led to a 1.4 ± 0.1-fold increase in scFv production as determined by labeling of the carboxy-terminal c-*myc* epitope. Table I presents a summary of the secretion optimization study indicating the substantial improvement in scFv yield.

Table I. Results of OX26 scFv Secretion Optimization

Expression system	Induction temperature (°C)	BiP	PDI	R261G	Secretion Level (μg/L)[a]
pRS-GALOX26	37	−	−	−	8
pRS-GALOX26	20	−	−	−	35
pRS-GALOX26	20	+	+	−	360
pITY-OX26	20	−	−	−	250
pITY-OX26	20	+	+	−	350
pRS-GALOX26	20	+	+	+	500

[a] Secretion levels were calculated using relative secretion data from Figs. 1–4 and the known purified yield of 500 μg/L.

Purification of OX26 scFv

The optimal yeast strain consisting of pRS-GALOX26 (R261G) with BiP and yeast PDI overexpression was used for secretion and batch purification of scFv. Expression was induced at 20°C for 3 days and 50 mL of the cell-free supernatant was used for scFv purification. After dialysis of the yeast supernatant, the scFv was purified using the carboxy-terminal six histidine epitope and nickel-NTA column chromatography (Materials and Methods). The purification process enriched the scFv to nearly 50% of the total protein (Fig. 5A, lane 4), and the purified yield was determined to be 0.5 mg/L (Table I). The second major protein species is an endogenous yeast protein that is regularly copurified from supernatants generated by yeast that are producing other scFvs or green fluorescent protein (data not shown).

Analysis of the purified protein indicated that the OX26 R261G scFv was full-length and that both the amino- and carboxy-termini were intact. The molecular weight of the purified scFv as determined by MALDI-TOF mass spectrometry was 29,586 (compared with the calculated theoretical molecular weight of 29,730). Mass spectrometry peptide mapping studies identified multiple tryptic peptides that were predicted to be present in the mature OX26 scFv based on the known amino acid sequence (data not shown). One of the tryptic peptides included the full carboxy-terminal six histidine epitope, confirming the presence of an intact carboxy terminus for the purified OX26 scFv. As indicated by the single OX26 band present on both the Coomassie-stained gel and Western blot (Fig. 5A, B), the N-terminus of the scFv was fully processed with complete removal of the pro

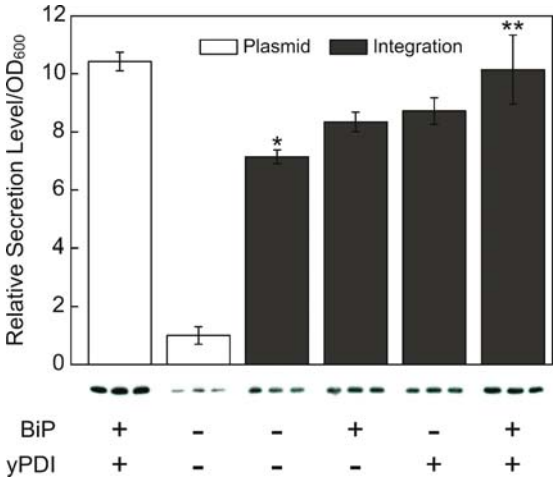

Fig. 4. Comparison of OX26 scFv secretion levels between plasmid-based and chromosomal integration-based expression systems and the effects of BiP and yPDI (pCT37) overexpression. Secretion levels were normalized to that of the plasmid-based wild-type yeast system (no BiP or yPDI cooverexpression). Induction temperature was 20°C. Statistical significance of the increases in secretion generated by the integration system with BiP and PDI cooverexpression (**) *vs.* the integration system alone (*) was determined by the statistical *t* test as $p < 0.001$.

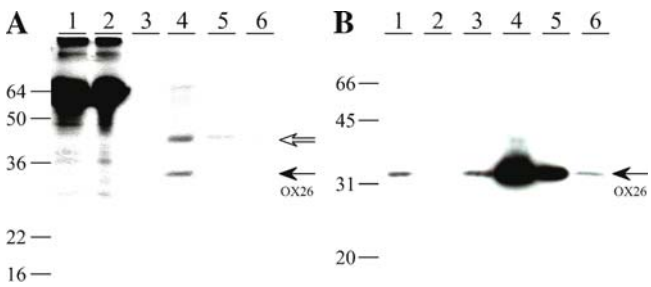

Fig. 5. Purification of OX26 R261G scFv using optimized secretion system with BiP and yPDI cooverexpression and 20°C induction. OX26 R261G scFv was purified using immobilized nickel agarose. (A) Coomassie-stained SDS-PAGE gel of purification products. (B) Western blot using anti-c-*myc* antibody. For both (A) and (B), lane 1: culture supernatant; lane 2: column flow-through; lanes 3–6: successive column elution fractions. Arrow indicates OX26 R261G scFv. Double arrow indicates general yeast supernatant protein that copurifies on nickel resin. Molecular masses are given in kDa to the left of each panel.

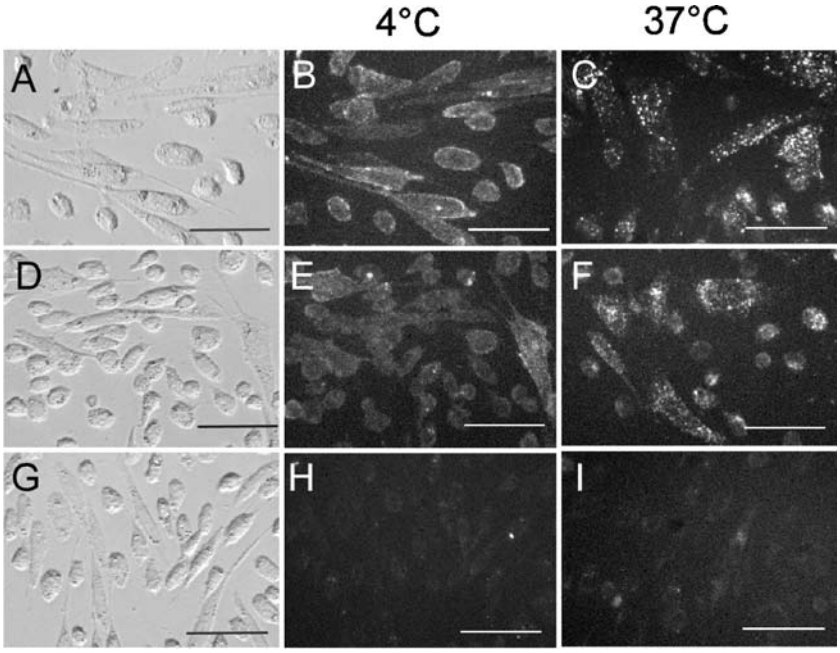

Fig. 6. OX26 scFv activity demonstrated by immunofluorescent labeling of and internalization into RBE4 cells. RBE4 cells were labeled by OX26 monoclonal antibody (A – C), purified OX26 scFv as artificial dimer (D–F), or purified irrelevant 4-4-20 scFv as artificial dimer (G–I), followed by phycoerythrin-conjugated secondary antibody at 4°C. The cells were then fixed and imaged (4°C samples), or incubated at 37° for 30 min to allow internalization prior to fixation and imaging (37°C samples). Phase contrast images and 4°C sample images correspond to the same microscope field, whereas 37°C images originate from a different sample. Scale bar: 50 μm.

region. N-terminal amino acid sequencing of the purified OX26 scFv further confirmed that the amino-terminus of the protein was correctly processed to its predicted mature form with complete removal of the pro region. Finally, the purified protein was treated with glycosidases and examined by Western blot (PNGase F and EndoHf for *N*-linked glycans, and α-mannosidase for removal of mannose residues from either *N*- or *O*-linked glycans). Neither *N*- nor *O*-glycosylation was detected as the untreated and glycosidase-treated scFv exhibited identical gel migration patterns (data not shown).

Functional Testing of OX26 scFv

To confirm that the yeast-produced OX26 scFv was active, the purified scFv was used for functional assays of cell surface binding and internalization. Live rat brain endothelial cells (RBE4 cell line) were probed with OX26 at 4°C to promote cell surface labeling of the transferrin receptor. The intact OX26 monoclonal antibody and the purified OX26 scFv labeled the surface of living RBE4 cells, whereas an irrelevant scFv against fluorescein (4-4-20) yielded no labeling (compare Fig. 6B, E, and H). Isotype control monoclonal antibody IgG2a also yielded no cell surface labeling (data not shown). When RBE4 cells were labeled at 4°C and then shifted to 37°C for 30 min, the OX26 monoclonal and OX26 scFv antibodies were internalized into punctate intracellular compartments indicative of endocytotic processing, whereas the control 4-4-20 scFv did not bind or internalize (Fig. 6C, F, I).

DISCUSSION

In this study, the OX26 scFv against the rat transferrin receptor was produced in *S. cerevisiae* at purified yields of 0.5 mg/L by using an optimal combination of gene dosage and manipulation of the yeast endoplasmic reticulum. BiP and PDI co-overexpression substantially increased the expression level, while 20°C production temperatures further enhanced expression. The scFv was secreted to the yeast supernatant as a soluble product that was fully processed to the expected uniform size. The purified scFv was proven active, and performed similarly to the MAb in terms of brain endothelial cell surface binding and internalization via the transferrin receptor transport system.

Previous studies have indicated that the OX26 scFv and OX26 scFv–streptavidin fusion were produced in the form of insoluble inclusion bodies in bacteria (19). The scFv product required denaturation of the inclusion bodies and protein refolding to produce active scFv protein. These processes increase the difficulty of scFv production and do not guarantee that the refolded scFv will be active. In contrast, the scFv produced by *S. cerevisiae* in this investigation is secreted in an active form to the yeast culture medium. Unlike the situation with bacterial expression systems, the eukaryotic quality control apparatus helps to ensure that high fidelity product, rather than large protein aggregates, is secreted (33). This beneficial yeast attribute is demonstrated by the effective cell labeling and internalization observed with the OX26 scFv without any requirement for denaturation and refolding.

Western blotting, molecular weight determination, peptide mapping, and N-terminal sequencing indicated that the scFv produced using the optimized *S. cerevisiae* expression system was the expected full-length protein having completely processed signal peptide. In contrast, attempts to produce the same scFv in *P. pastoris* resulted in partial retention of the α-factor pro region. In addition, the *P. pastoris*-produced scFv was heterogeneously glycosylated as a result of the α-factor pro region having three endogenous *N*-glycosylation sites. Yeast glycosylation patterns are potentially immunogenic and therefore such heterogeneous glycosylation is undesirable. Optimization of medium pH helped reduce, but did not fully eliminate, the unprocessed and glycosylated scFv material (20). Importantly, the pro region employed here is a synthetic pro region that is based on the α-factor pro region, but lacks the *N*-linked glycosylation sites. Thus as expected, the purified scFv was not *N*-glycosylated because both the scFv and leader sequence lack putative *N*-linked glycosylation sites. In addition, *O*-linked glycosylation of the purified scFv was not detected. Although the synthetic pro region lacks glycosylation, it retains the necessary characteristics for protein processing through the secretory pathway and was shown to mediate the same expression levels of human epidermal growth factor when compared with the native α-factor leader (32). This synthetic pro region has also been used in the expression of other scFvs (16,17), single-chain T-cell receptors (23), GFP (29), and G-protein coupled receptors (34).

The optimization of the yeast protein folding environment was successful in raising scFv secretion levels by approximately 10-fold. BiP was originally identified in association with antibody heavy chains and acts as a protein folding chaperone by binding to exposed hydrophobic patches (35). On the other hand, protein disulfide isomerase can act in the formation of disulfide linkages and in the isomerization of nonnative disulfide bonds (36). Single-chain antibodies have an inherent insolubility as a result of the removal of the antibody constant regions that leaves newly solvent-exposed regions on the variable chains (14). In addition, scFvs have two disulfide bonds, one in each of the variable light and heavy chains. Cooverexpression of BiP and PDI also increases the expression of other scFvs in yeast (17). The increased expression of OX26 scFv is likely a result of PDI isomerase activity and the ability of BiP to prevent premature aggregation and degradation by the yeast quality control apparatus (17). OX26 scFv seems particularly prone to aggregation as indicated by both the aforementioned bacterial expression studies and the benefits of BiP and PDI overexpression in this study.

Liposomes decorated with OX26 MAb have been successfully transported across an *in vitro* model of the BBB consisting of confluent RBE4 cell monolayers (9). In addition, as Fig. 6 demonstrates, the unconjugated OX26 MAb can mediate internalization of RBE4 cells into putative endosomal compartments. OX26 scFv performs similarly to the MAb in terms of qualitative labeling intensity at similar labeling concentrations (10 μg/mL for MAb, and 2.4 μg/mL for scFv). The bacterially produced OX26 scFv–streptavidin fusion also performed similarly to the MAb *in vivo* (19); this indicates that the scFv could be a viable brain targeting and transport moiety.

The facile expression of soluble and active OX26 scFv using the methods described here has several potential implications. First, this particular scFv targets the transferrin receptor transcytosis system as a surrogate ligand that allows transport into brain endothelial cells *in vitro* and across the BBB endothelium *in vivo*. In addition, the brain targeting and delivery attributes of OX26 scFv could allow for effective targeting of drug-loaded liposomes or nanoparticles to the brain microvasculature. Also, recombinant expression of scFv–protein therapeutic fusions may be possible given that an OX26 scFv–green fluorescent protein fusion has been secreted using this system (E.V. Shusta, unpublished results). Such bifunctional protein molecules would have the potential for noninvasive brain uptake with the OX26 scFv mediating BBB transport and the fused protein cargo inducing pharmacological responses in brain tissue. Finally, the optimized yeast expression system could likely be used for production of other scFvs identified for their targeting and delivery attributes.

ACKNOWLEDGMENTS

Special thanks are extended to Grzegorz Sabat, James Brown, and Dr. Amy Harms of the University of Wisconsin Biotechnology Center for their assistance in analyzing peptide mapping and intact protein molecular weight measurement data. Thanks are also due to Michael Pereckas at the Medical College of Wisconsin for his assistance with protein sequencing. This study was funded by the Whitaker Foundation award RG-02-0077 and NSF CAREER award BES-0238864. B.J. Hackel was an NSF REU recipient and a University of Wisconsin Hilldale undergraduate research fellow.

REFERENCES

1. W. M. Pardridge. The blood–brain barrier: bottleneck in brain drug development. *Neurorx* **2**:3–14 (2005).
2. H. Sun, H. Dai, N. Shaik, and W. F. Elmquist. Drug efflux transporters in the CNS. *Adv. Drug. Deliv. Rev.* **55**:83–105 (2003).
3. W. M. Pardridge, J. Eisenberg, and J. Yang. Human blood–brain barrier insulin receptor. *J. Neurochem.* **44**:1771–1778 (1985).
4. J. B. Fishman, J. B. Rubin, J. V. Handrahan, J. R. Connor, and R. E. Fine. Receptor-mediated transcytosis of transferrin across the blood–brain barrier. *J. Neurosci. Res.* **18**:299–304 (1987).
5. P. M. Friden, L. R. Walus, G. F. Musso, M. A. Taylor, B. Malfroy, and R. M. Starzyk. Anti-transferrin receptor antibody and antibody–drug conjugates cross the blood–brain barrier. *Proc. Natl. Acad. Sci. USA* **88**:4771–4775 (1991).
6. P. M. Friden, L. R. Walus, P. Watson, S. R. Doctrow, J. W. Kozarich, C. Backman, H. Bergman, B. Hoffer, F. Bloom, and A. C. Granholm. Blood–brain barrier penetration and *in vivo* activity of an NGF conjugate. *Science* **259**:373–377 (1993).
7. Y. Zhang and W. M. Pardridge. Neuroprotection in transient focal brain ischemia after delayed intravenous administration of brain-derived neurotrophic factor conjugated to a blood–brain barrier drug targeting system. *Stroke* **32**:1378–1384 (2001).
8. B. W. Song, H. V. Vinters, D. Wu, and W. M. Pardridge. Enhanced neuroprotective effects of basic fibroblast growth factor in regional brain ischemia after conjugation to a blood–brain barrier delivery vector. *J. Pharmacol. Exp. Ther.* **301**:605–610 (2002).
9. A. Cerletti, J. Drewe, G. Fricker, A. N. Eberle, and J. Huwyler. Endocytosis and transcytosis of an immunoliposome-based brain drug delivery system. *J. Drug Target.* **8**:435–446 (2000).
10. N. Shi, Y. Zhang, C. Zhu, R. J. Boado, and W. M. Pardridge.

Brain-specific expression of an exogenous gene after i.v. administration. *Proc. Natl. Acad. Sci. USA* **98**:12754–12759 (2001).
11. Y. Zhang, F. Schlachetzki, Y. F. Zhang, R. J. Boado, and W. M. Pardridge. Normalization of striatal tyrosine hydroxylase and reversal of motor impairment in experimental parkinsonism with intravenous nonviral gene therapy and a brain-specific promoter. *Hum. Gene Ther.* **15**:339–350 (2004).
12. Y. Zhang, F. Schlachetzki, and W. M. Pardridge. Global nonviral gene transfer to the primate brain following intravenous administration. *Mol. Ther.* **7**:11–18 (2003).
13. J. C. Olivier, R. Huertas, H. J. Lee, F. Calon, and W. M. Pardridge. Synthesis of pegylated immunonanoparticles. *Pharm. Res.* **19**:1137–1143 (2002).
14. L. Nieba, A. Honegger, C. Krebber, and A. Plückthun. Disrupting the hydrophobic patches at the antibody variable/constant domain interface: improved *in vivo* folding and physical characterization of an engineered scFv fragment. *Protein Eng.* **10**:435–444 (1997).
15. P. Carter, R. F. Kelley, M. L. Rodrigues, B. Snedecor, M. Covarrubias, M. D. Velligan, W. L. T. Wong, A. M. Rowland, C. E. Kotts, M. E. Carver, M. Yang, J. H. Bourell, H. M. Shepard, and D. Henner. High level *Escherichia coli* expression and production of a bivalent humanized antibody fragment. *Bio/Technology* **10**:163–167 (1992).
16. M. J. Feldhaus, R. W. Siegel, L. K. Opresko, J. R. Coleman, J. M. Feldhaus, Y. A. Yeung, J. R. Cochran, P. Heinzelman, D. Colby, J. Swers, C. Graff, H. S. Wiley, and K. D. Wittrup. Flow-cytometric isolation of human antibodies from a nonimmune Saccharomyces cerevisiae surface display library. *Nat. Biotechnol.* **21**:163–170 (2003).
17. E. V. Shusta, R. T. Raines, A. Pluckthun, and K. D. Wittrup. Increasing the secretory capacity of *Saccharomyces cerevisiae* for production of single-chain antibody fragments. *Nat. Biotechnol.* **16**:773–777 (1998).
18. M. A. Poul, B. Becerril, U. B. Nielsen, P. Morisson, and J. D. Marks. Selection of tumor-specific internalizing human antibodies from phage libraries. *J. Mol. Biol.* **301**:1149–1161 (2000).
19. J. Y. Li, K. Sugimura, R. J. Boado, H. J. Lee, C. Zhang, S. Duebel, and W. M. Pardridge. Genetically engineered brain drug delivery vectors: cloning, expression and *in vivo* application of an anti-transferrin receptor single chain antibody–streptavidin fusion gene and protein. *Protein Eng.* **12**:787–796 (1999).
20. R. J. Boado, A. Ji, and W. M. Pardridge. Cloning and expression in Pichia pastoris of a genetically engineered single chain antibody against the rat transferrin receptor. *J. Drug Target.* **8**:403–412 (2000).
21. R. D. Gietz, R. H. Schiestl, A. R. Willems, and R. A. Woods. Studies on the transformation of intact yeast cells by the LiAc/SS-DNA/PEG procedure. *Yeast* **11**:355–360 (1995).
22. A. S. Robinson, V. Hines, and K. D. Wittrup. Protein disulfide isomerase overexpression increases secretion of foreign proteins in *Saccharomyces cerevisiae*. *Bio/Technology* **12**:381–384 (1994).
23. E. V. Shusta, P. D. Holler, M. C. Kieke, D. M. Kranz, and K. D. Wittrup. Directed evolution of a stable scaffold for T-cell receptor engineering. *Nat. Biotechnol.* **18**:754–759 (2000).
24. R. N. Parekh, M. R. Shaw, and K. D. Wittrup. An integrating vector for tunable high copy stable integration into the dispersed Ty δ sites of *Saccharomyces cerevisiae*. *Biotechnol. Prog.* **12**:16–21 (1996).
25. M. C. A. Laboissiere, S. L. Sturley, and R. T. Raines. The essential function of protein disulfide isomerase is to unscramble non-native disulfide bonds. *J. Biol. Chem.* **47**:28006–28009 (1996).
26. A. S. Robinson, J. A. Bockhaus, A. C. Voegler, and K. D. Wittrup. Reduction of BiP levels decreases heterologous protein secretion in *Saccharomyces cerevisiae*. *J. Biol. Chem.* **271**:10017–10022 (1996).
27. C. Tachibana and T. H. Stevens. The yeast EUG1 gene encodes an endoplasmic reticulum protein that is functionally related to protein disulfide isomerase. *Mol. Cell. Biol.* **12**:4601–4611 (1996).
28. R. S. Sikorski and P. Hieter. A system of shuttle vectors and yeast host strains designed for efficient manipulation of DNA in *Saccharomyces cerevisiae*. *Genetics* **122**:19–27 (1989).
29. D. Huang and E. V. Shusta. Secretion and surface display of green fluorescent protein using the yeast *Saccharomyces cerevisiae*. *Biotechnol. Prog.* **21**:349–357 (2005).
30. F. Roux, O. Durieu-Trautmann, N. Chaverot, M. Claire, P. Mailly, J. M. Bourre, A. D. Strosberg, and P. O. Couraud. Regulation of gamma-glutamyl transpeptidase and alkaline phosphatase activities in immortalized rat brain microvessel endothelial cells. *J. Cell. Physiol* **159**:101–113 (1994).
31. X. Wang, M. Campoli, E. Ko, W. Luo, and S. Ferrone. Enhancement of scFv fragment reactivity with target antigens in binding assays following mixing with anti-tag monoclonal antibodies. *J. Immunol. Methods* **294**:23–35 (2004).
32. J. M. Clements, G. H. Catlin, M. J. Price, and R. M. Edwards. Secretion of human epidermal growth factor from *Saccharomyces cerevisiae* using synthetic leader sequences. *Gene* **106**:267–271 (1991).
33. C. Hammond and A. Helenius. Quality control in the secretory pathway. *Curr. Opin. Cell Biol.* **7**:523–529 (1991).
34. J. A. Butz, R. T. Niebauer, and A. S. Robinson. Co-expression of molecular chaperones does not improve the heterologous expression of mammalian G-protein coupled receptor expression in yeast. *Biotechnol. Bioeng.* **84**:292–304 (2003).
35. J. Ma, J. F. Kearney, and L. M. Hendershot. Association of transport-defective light chains with immunoglobulin heavy chain binding protein. *Mol. Immunol.* **27**:623–630 (1990).
36. H. Gilbert. Protein disulfide isomerase and assisted protein folding. *J. Biol. Chem.* **272**:29399–29402 (1997).